Critical thickness for the agglomeration of thin metal films

C. Boragno,[1] F. Buatier de Mongeot,[1] R. Felici,[2] and I. K. Robinson[3]
[1]*Dipartimento di Fisica, Università di Genova, Via Dodecaneso 33 Genova, Italy*
[2]*European Synchrotron Radiation Facility, BP 220, F-38043 Grenoble, France*
[3]*University College London, Gower Street, London WC1E 6BT, United Kingdom*
(Received 10 July 2008; revised manuscript received 22 December 2008; published 27 April 2009)

A thin metal film can exist in a metastable state with respect to breaking into small clusters. In this paper we report on grazing incidence small-angle x-ray scattering studies carried out *in situ* during the annealing of thin Ni films, between 2 and 10 nm thick, deposited on an amorphous SiO_2 substrate. Our results show the presence of two different regimes which depend on the initial film thickness. For thicknesses less than 5 nm the annealing results in the formation of small, compact clusters on top of a residual Ni wetting layer. For thicknesses greater than 5 nm the film breaks into large, well-separated clusters and the substrate shows an uncovered clean surface.

DOI: 10.1103/PhysRevB.79.155443 PACS number(s): 61.05.C−, 68.55.−a, 61.46.Df, 81.07.−b

I. INTRODUCTION

A thin, solid, homogeneous, metallic film deposited on an inert, amorphous substrate can break into droplets (clusters) when sufficient activation energy is provided. This phenomenon, known as agglomeration or dewetting, is technologically important in the microelectronics industry, as it can be responsible for the breaking of electrical interconnections, but it is also studied as one of the methods of producing arrays of nanosized metal clusters.[1] Agglomeration of polycrystalline films is a mass transport process that uncovers the surface of the substrate in order to reduce the total free energy of the system.

In a different context, the principal source of the behavior was identified in 1958 by Mullins[2] as an instability of the point at which the grain boundaries emerge from the surface of the film. In many cases, a temperature of a few hundred °C, well below the melting point of the metal, is sufficient to cause the rupture of the film.[3,4] At the end of the process, a disordered arrangement of three-dimensional (3D) nanometric or micrometric islands is present on the substrate whose spatial distribution can be controlled by using nanopatterned substrates.[5] This nonequilibrium phenomenon is of interest for potential technological applications, in nonlinear optics and nanophotonics[6,7] as well as in catalysis.[8,9]

Many experimental studies have been carried out on the agglomeration of thin metal films deposited on inert substrates. However, among the different techniques adopted, real-time methods have rarely been applied to this problem. As an example, some information on the dynamics can be obtained by measuring resistivity,[3] but this method only provides information on the final part of the process when the film has already started to break down.

In this paper, we present a study of this phenomenon by using *in situ* grazing incidence small angle x-ray scattering (GISAXS). This technique is able to provide detailed information on the morphology, shape, and correlation of surfaces and/or clusters grown at surfaces,[10] and then can be applied for studying, in real time, the morphological evolution of a metal film during the agglomeration process. This kind of information has not previously been accessible, and the final or intermediate morphology have so far been analyzed by microscopy studies.[4,11]

II. RESULTS

The system under study is made of a Ni film deposited onto an amorphous SiO_2 substrate. This system is important as it is often used as a catalyst for the growth of carbon nanotubes via thermal cracking of C-based gases (methane, ethylene).[9]

The experiment has been carried out at the 34–ID-C beamline of the Advanced Photon Source (APS), in Chicago (USA). This beamline has the peculiarity of allowing the x-ray beam to reach the sample without crossing any Be window limiting the diffused background. This is crucial when it is necessary to measure the small signal due to the presence of nanoclusters, whose scattering intensity is comparable with the diffuse scattering of a Be window. The clean silicon wafer substrates were inserted into the UHV chamber (base pressure $<10^{-9}$ torr) and Ni films were then deposited *in situ* by an e-beam evaporator, maintaining the substrate at 100 °C in order to improve the homogeneity of the film. It is important to note that deposition at slightly higher temperatures (~150 °C) results in the immediate formation of clusters without passing through a homogeneous film state.

The samples were heated by a ceramic heater, while the temperature was measured by a thermocouple placed on the sample clip. The accuracy in T was estimated to be 10 °C. For all the measured samples, the incident photon energy was fixed at 8 keV ($\lambda=0.155$ nm) and, in the case of the GISAXS measurements, the incidence angle, with respect to the sample surface, was 1°. At this photon energy, the critical angles for Ni and SiO_2 are 0.4° and 0.21°, respectively. GISAXS intensities were recorded using a Princeton charge-coupled device (CCD) camera placed on the diffractometer arm at a distance of 1420 mm from the sample, giving an angular resolution of 0.0018° or a wave-vector resolution of 1.27×10^{-4} A^{-1} in both directions, perpendicular and parallel to the sample surface.

For all samples, the experimental procedure was the following: after checking the substrate reflectivity, we measured

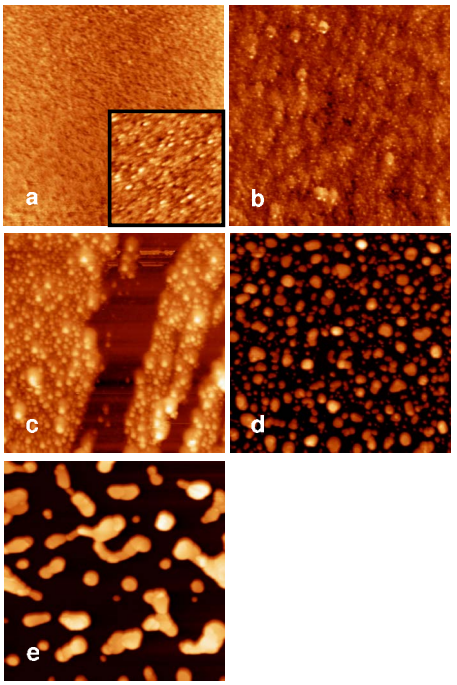

FIG. 1. (Color online) Final morphologies measured by *ex situ* AFM on Ni films with different initial thicknesses: (a) 1.8 nm; (b) 3.7 nm ; (c) 5.2 nm ; (d) 7.6 nm ; (e) 10.1 nm. Image size: 8 $\times 8$ μm^2 for a,d,e; 4×4 μm^2 for b,c and 500×500 nm^2 for the inset in (a).

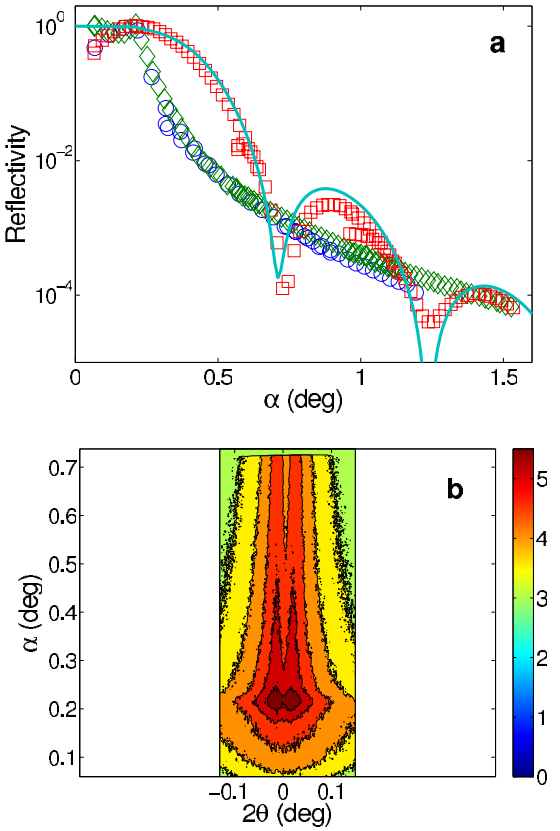

FIG. 2. (Color online) X-ray reflectivity curves (a) acquired on the bare substrate (circles), on the as-deposited Ni film (squares) and on the agglomerated film (diamonds) for sample S2. The continuous line is the fit for the as-deposited film. In (b), the GISAXS map acquired on the agglomerated film is presented (logarithmic intensity scale) as a function of the in-plane scattering angle 2θ and out-of-plane angle α.

the x-ray intensity under specular reflection conditions for a reflectivity angle of 2° as function of the deposition time, in order to monitor the Ni growth. This measurement, similar in concept to the *in situ* reflection high-energy electron-diffraction (RHEED) measurements, allows an exact control of the film thickness during deposition.

After deposition, we measured the reflectivity of the Ni film before the annealing procedure to exactly determine the thickness and density of the metal film together with its surface roughness.[12] Then we performed the GISAXS measurements, with an x-ray incidence angle of 1°, while increasing the substrate temperature in steps (maximum temperature around 700 K) and monitoring the GISAXS intensity in real time. GISAXS intensity maps are collected as a function of the 2θ in-plane angle and as a function of the x-ray exit angle α perpendicular to the surface. At the end of the annealing procedure (typical annealing time around 10 000 s), we again measured the specular reflectivity and finally the surface morphology by *ex situ* atomic force microscopy (AFM).

In Fig. 1 we report the final morphology (i.e., after the annealing procedure) of several Ni films with thicknesses in the range 1.8–10 nm. The pristine thickness of the films was 1.8, 3.7, 5.2, 7.6, and 10.1 nm from top-left to bottom-right, respectively, as determined by x-ray reflectivity. AFM measurements indicate a roughness (peak to peak) of around 2 and 3 nm for the samples a and b, respectively, a film thickness (in relation to the substrate) of around 20 nm for sample c and an island height in the range of 30–60 nm and 60–80 nm for the samples d and e, respectively. From these images it is evident that the system evolves following two different regimes: thin films (panels a and b) remain compact, with nanometric protrusions and without exposing the SiO_2 substrate, while thick films (panels d and e) break into well-separated islands. An intermediate morphology can be observed for a film thickness of about 5 nm [Fig. 1(c)].

In the following, we present a detailed analysis of x-ray measurements for two representative samples, known hereafter as S1 and S2, corresponding to the panels b and d of Fig. 1, respectively.

Figure 2(a) shows the measured reflectivity curves, before and after the annealing procedure, for the S2 sample. By fitting the reflectivity curve obtained on the as-deposited film, we infer a thickness of 7.6 nm with a mean roughness of 0.6 nm, comparable to that of the SiO_2 substrate.

At the end of the agglomeration process, large Ni clusters are present on the substrate [cf. Fig. 1(d)], while the reflectivity curve is quite similar to that measured on the pristine substrate [diamonds and open circles in Fig. 2(a)], indicating that the main contribution to the x-ray reflected intensity comes from the uncovered SiO_2 substrate. It should be noted that the two curves have been normalized to 1 in the total reflection region. The two normalization coefficients are different and, in particular, one of the curve obtained after annealing is larger indicating a smaller surface area consistent with the partial coverage due to the metal clusters. A typical

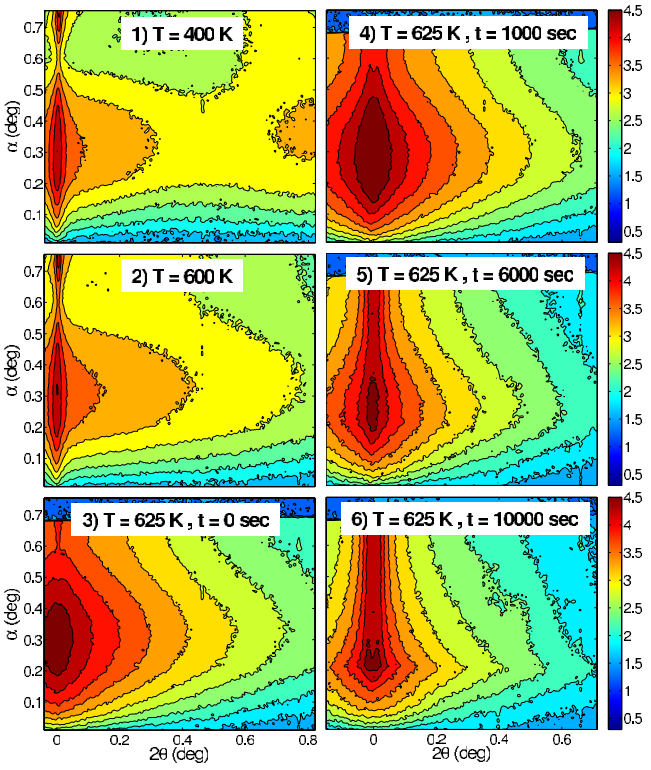

FIG. 3. (Color online) GISAXS maps acquired at different stages of the annealing procedure for sample S2. The temperature T and the time t at which the sample was kept before measuring the GISAXS intensity maps are indicated in the figures.

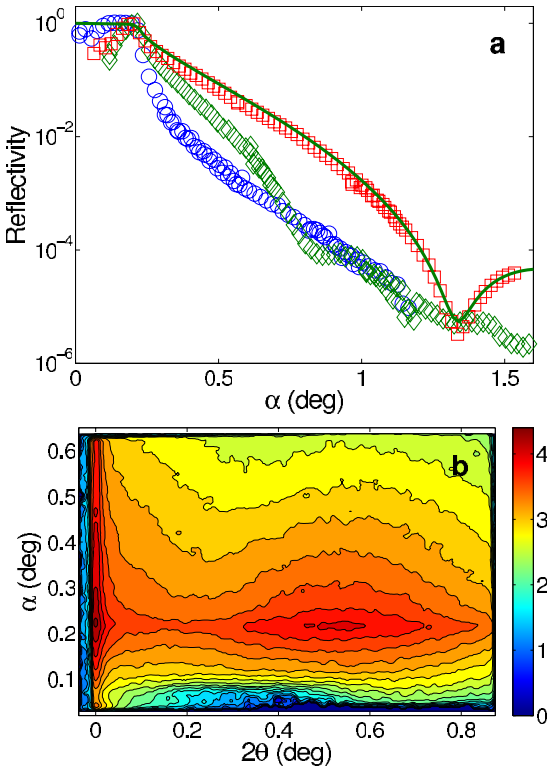

FIG. 4. (Color online) X-ray reflectivity curves (a) acquired on the bare substrate (circles), on the as-deposited Ni film (squares) and on the agglomerated film (diamonds) for sample S1. The continuous line is the fit for the as-deposited film. In (b), the GISAXS intensity map acquired on the agglomerated film is presented (logarithmic intensity scale)

GISAXS intensity map, taken when the film was already agglomerated, is presented in Fig. 2(b): two clearly resolved shoulders, around the specular plane, indicate the presence of Ni islands spatially distributed on the substrate.[10] The intensity has a maximum in correspondence of the exit angle $\alpha = 0.21°$, corresponding to the SiO_2 critical angle, indicating that the substrate is largely uncovered, in agreement with the AFM analysis.

In order to follow the film evolution in real time, we acquired GISAXS intensity maps with an integration time of 40 s, while increasing the temperature in steps from room temperature (RT) to 650 K.

Figure 3 collects some examples of GISAXS maps acquired during the annealing procedure. All the maps are presented in the same logarithmic color scale.

At the beginning, [Fig. 3-1], the GISAXS intensity map presents only a weak signal at $2\theta \sim 0.8°$ indicating a short-range disorder typical for the pristine Ni film. At 600 K [Fig. 3-2], this original disorder disappears, and the film becomes smoother. Maintaining the film at this temperature does not induce any surface morphology modification with time in the 600 s interval we followed the evolution. The situation is quite different if the temperature is raised to 625 K [Fig. 3-3] where a fast, strong increase in the scattered intensity is observed. With time, the shape of the scattered intensity evolves [Figs. 3-4 and 3-5] and finally [Fig. 3-6] two clearly resolved shoulders appear in the GISAXS intensity map, indicating the presence of separated objects with a well-defined spatial correlation.

It is also interesting to note the dependence in α of the diffused intensity. At the beginning, the diffused intensity has its maximum for $\alpha \sim 0.3°$ [Fig. 3-3] corresponding to the critical value for total reflection of the 5.2 nm thick Ni film. The position of this maximum changes from 0.3° to 0.21° corresponding to the clean silicon oxide substrate [Fig. 3-6]. This observation is an indication for the reference surface of the GISAXS pattern. At the beginning, the reference surface is the Ni-air interface indicating that the grooves start forming at this interface. These become larger and deeper until they reach the substrate. At this point, the real agglomeration process starts. The film breaks up and clusters form. From the point of view of the GISAXS intensity, this corresponds to the classic situation of a surface covered with well-separated clusters. The reference surface is then the substrate one and the diffused intensity has its maximum at the critical angle value of the silicon oxide ($\alpha \sim 0.21°$).

This process takes a long time to be completed, at least 7000 s at 625 K. In this time, islands assume a stable configuration, either in distance or in dimension, in the sense that no further evolution is measurable.

We observed a completely different behavior in films with thicknesses of less than about 5 nm. In Fig. 4 we report, in analogy with Fig. 2, the reflectivity curves and the GISAXS map of the final status for the sample S1. From the fit of the pristine film [squares in Fig. 4(a)] we determined a film thickness of 3.5 nm with a mean roughness of 0.6 nm. The

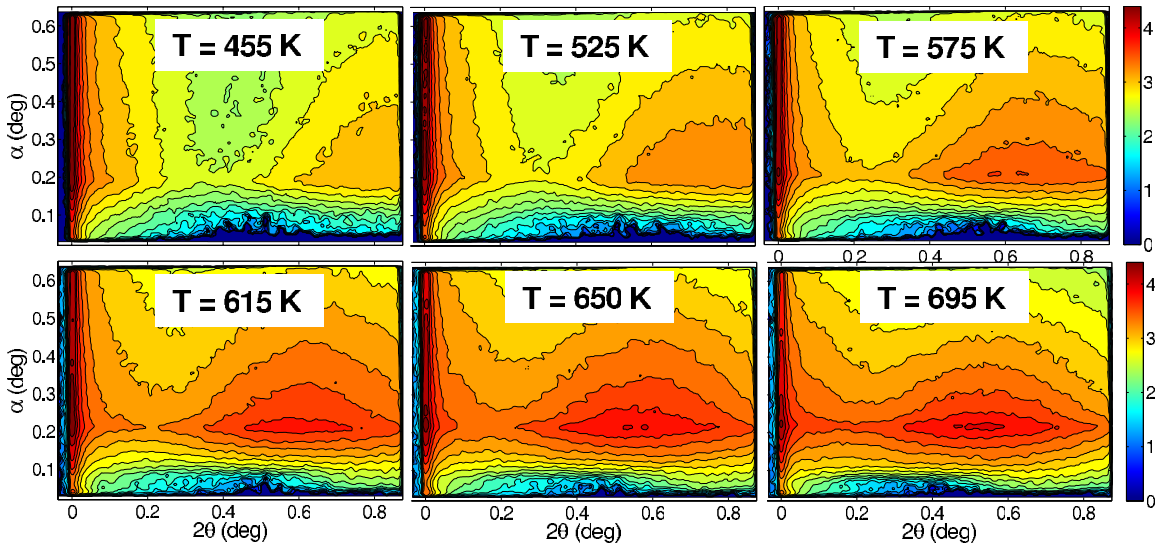

FIG. 5. (Color online) GISAXS intensity maps acquired at different stages of the annealing procedure for sample S1.

reflectivity curve of the annealed film [diamonds in Fig. 4(a)] is now quite different from the curve of the bare substrate, as observed for the S2 sample [Fig. 2(a)]. The shape of the curve and the local minimum at $\alpha \sim 0.8°$ suggest that the average film thickness is 6.8 nm, greater than the initial value. However it is not possible to fit this reflectivity curve with a simple model based on a homogeneous layer and a normal surface roughness and this is an indication of the complicated surface morphology of the film.

The GISAXS intensity map of the final state [Fig. 4(b)] is quite different in respect to the previous case: a shoulder is evident, but its center is at a very large angle ($2\theta \sim 0.5°$). The different behavior is even more evident by following the temperature-time evolution of the GISAXS intensity maps, as reported in Fig. 5.

The main difference in respect to the previous case is that now the driving force is the temperature, not the time: fixing T at a value and following the time evolution of the GISAXS intensity map, we did not observe any relevant difference, at least for the time we followed the evolution (about 1 h). But a change in T causes a fast change in the GISAXS maps as well (just a few minutes). The other important result is that the scattered intensity does not show the "explosive" behavior reported in the previous case, but it increases slowly throughout the process. That means the Ni film maintains its original structure and therefore no drastic changes in morphology happen, only a smooth evolution toward new equilibrium configurations.

In order to easily compare the two different behaviors, we collected from each GISAXS intensity map the intensity profile as a function of 2θ for the exit angle $\alpha = 0.21°$, obtaining a plot in which the vertical axis is time. Such plots are presented for both samples in Fig. 6.

Summarizing our results, we observed in real time, using the GISAXS technique, the evolution of Ni films deposited onto SiO_2 substrates, evidencing the existence of two different behaviors, depending on the initial film thickness. In the following, we propose a model to interpret these results.

III. DISCUSSION

Let us first consider the time-temperature evolution of the S2 sample.

Figure 6, left panel, suggests that at $T \sim 625$ K a dramatic change happens: the intensity grows rapidly around the specular beam [cf. Fig. 3-3] but there is no evidence for any

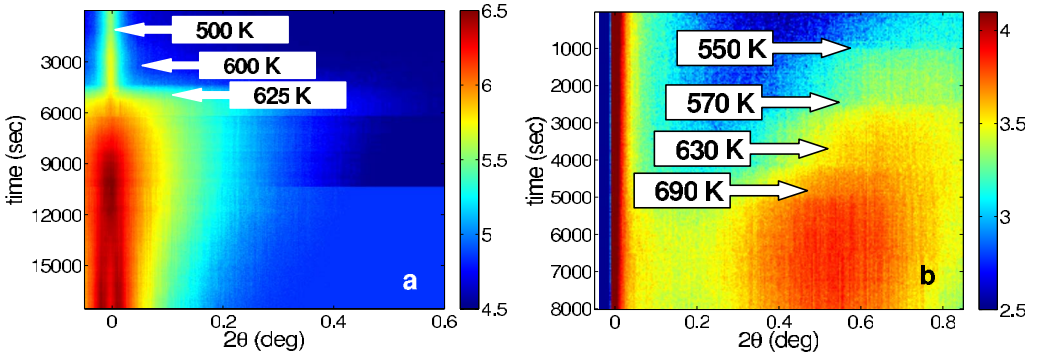

FIG. 6. (Color online) Time and temperature evolution for S2 (left) and S1 (right) samples. The maps have been constructed by plotting the intensity as a function of 2θ at the exit angle $\alpha = 0.21°$ from each GISAXS intensity map as a function of time. The balloons mark the time at which the temperature was stabilized at a new value. The intensity maps are presented in a logarithmic color scale.

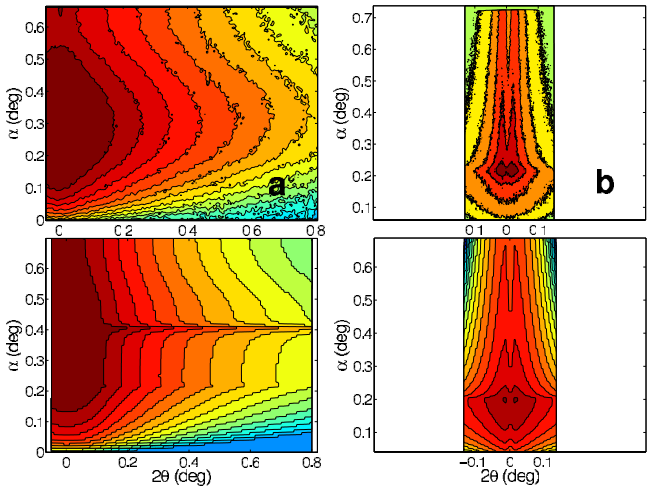

FIG. 7. (Color online) Experimental GISAXS intensity maps (top row) and corresponding simulations obtained with the ISGISAXS software (bottom row) for the S2 sample. The left column (a) corresponds to the Fig. 3-3 while the right column (b) corresponds to the Fig. 3-6.

lateral correlation of the surface roughness, which is instead clearly evident later on (after about 12 000 s).

In order to better understand this process, we tried to simulate the acquired GISAXS maps with a software usually used to interpret them, IsGISAXS.[13]

In Fig. 7 we present the two GISAXS intensity maps measured on the S2 sample at different annealing stages with the corresponding simulations. The bottom-left panel of Fig. 7 corresponds to the initial stage of the agglomeration process. The best fit was achieved by using a disordered array of holes, with a cylindrical shape, radius between 5 and 40 nm (log-normal distribution), height between 0.5 and 8 nm (Gaussian distribution) in a Ni film with thickness 8 nm. This simulation is able to replicate the main features of the acquired map (top-left panel): the intensity extends toward large values of the parallel exit angle; the intensity along the $2\theta=0°$ line is almost constant between $\alpha=0.21°$ and $\alpha=0.43°$. The two streaks as a function of 2θ at $\alpha=0.21°$ and $0.43°$ in the simulation are induced by the discontinuity in the reflectivity at the critical angles of Ni and SiO_2. Moreover the almost constant intensity as a function of α in the range $0.21°-0.43°$ is due to the cylindrical shape of the holes. Unfortunately we have not been able to find a suitable shape for this intermediate state when the holes start to form at the surface, however the cylindrical shape is the one giving the best fit.

In the same figure, in the bottom-right panel, we report the simulation of the S2 sample final status, when the film is completely agglomerated. The simulation has been done considering a log-normal distribution of hemispherical islands, having radius R between 8 and 200 nm and height equal to $0.12R$, dispersed on the substrate with an average distance of 370 nm. In this case, the simulation reflects much better the main feature of the observed GISAXS map, reported in the top-right panel.

The picture of the process in Fig. 3 coming out from this analysis is the following: at the beginning (low temperature) the reflected intensity at the SiO_2 critical angle is low, since the Ni film is compact and smooth. Upon increasing T, the intensity slowly rises, indicating an increasing of the film roughness, which is still not in-plane correlated. When the temperature reaches $T=625$ K, grooves start to appear at the film surface. These grooves increase in size and depth, until they touch the substrate surface. When the grooves merge, the film begins to break up into many islands, which evolve toward an equilibrium distribution in size and lateral separation.

This picture is in agreement with the model usually adopted for agglomeration:[14–16] the free surface of a film has the tendency of "grooving" between two adjacent grains by the formation of a depression along the boundary, as described in the original Mullins theory.[2] This tendency is typically justified as satisfying a force balance among the two surface-grain and the grain-grain interfacial tensions. A triple point, where three grains meet, represents a preferred site along the grooved grain boundary for heterogeneous nucleation of voids. Upon annealing a thin film, voids are formed that expose part of the substrate surface. With further annealing these voids grow and impinge upon each other, resulting in a porous yet partially continuous film. Further annealing eventually forms isolated islands of the film material. This "grain-boundary grooving" mechanism foresees that agglomeration can be prevented by reducing the grain size L or increasing the film thickness t

To model the behavior of sample S1 we again used IsGISAXS software.

The model used consists of hemispherical islands on top of a residual Ni wetting layer. In Fig. 8(a), we present a GISAXS map and the corresponding simulation (top and bottom, respectively). A good agreement is evident and since the model is simpler than the previous case, it is possible to follow the temperature evolution of the most relevant free parameters of the model, i.e., the thickness of the wetting layer d and the radius R of the particles [Fig. 8(b)]. Beyond the large statistical errors, the trend is clear: by increasing the temperature, more and more material is transferred from the wetting layer to the growing particles. The system evolves through equilibrium states, thermally activated, and thus there is no (or little) time evolution.

In order to interpret this behavior, we refer to a couple of papers by Rha and Park[16–18] which studied the agglomeration process of a metallic film deposited on an inert substrate. By minimizing the surface energy of such a system as a function of the film geometry, they demonstrated that the grooving mechanism can lead to the formation of an array of touching compact islands without the exposure of the substrate. This state is metastable and can evolve to a state with separated clusters if an energetic barrier is overcome. Our guess is that under our experimental conditions (temperature), the initially compact Ni film evolves toward this metastable state (cf. Fig. 6 in Ref. 18). However, to reach this film configuration we have to consider another mechanism: the movement of grain boundaries. As demonstrated by Rost *et al.*,[19] the annealing process causes an enlargement of the grain size and at the same time an increase in the surface curvature, which tends to assume the equilibrium configuration.

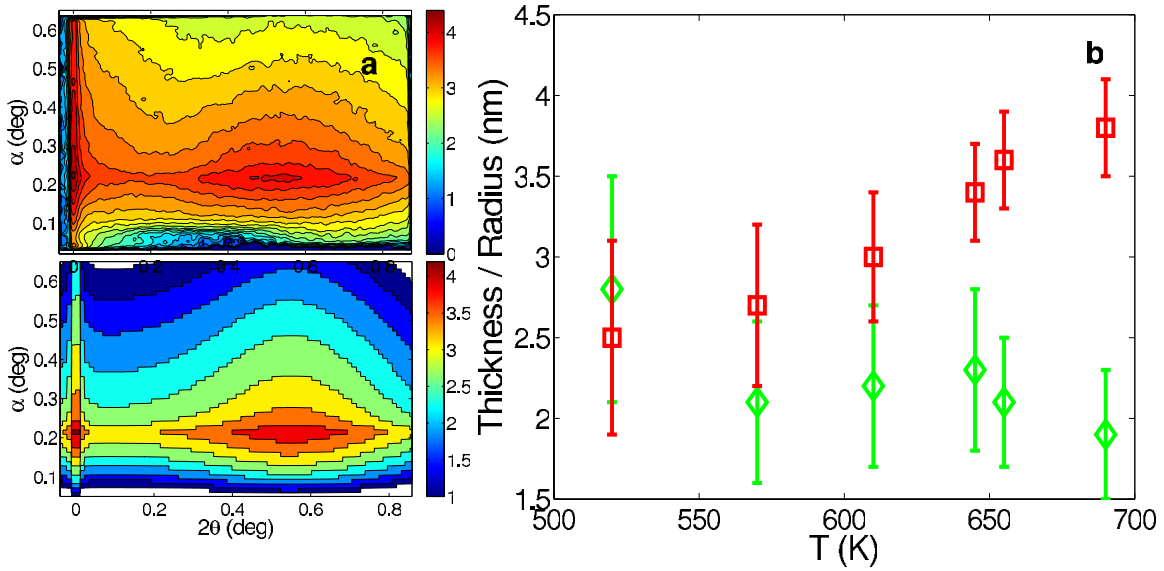

FIG. 8. (Color online) In (a) the experimental GISAXS intensity map and the corresponding simulation obtained with the ISGISAXS package for the final state of the S1 sample (top and bottom, respectively); in (b) the temperature evolution of the thickness of the wetting layer (diamonds) and of the particle radius (squares) (see text).

In thick films, these two effects cooperate with the grooving mechanism: the grain size and the local curvature increase as a function of temperature and when a critical value is reached, holes are formed at the grain boundaries and the film begins to break up into separated islands. On the contrary, in thin film, the enlargement of the grain size and the grain-boundary movement is inhibited or strongly reduced, and the surface curvature cannot reach the critical value. In this case, the grooves cannot reach the substrate and the film morphology is due to connected islands sitting on top of a wetting layer, like in the metastable regime described by Rha and Park.[18]

IV. CONCLUSIONS

We studied by a real-time method, GISAXS, the temperature and time evolution of metal films deposited on an inert amorphous substrate. From our measurements, two different regimes can be distinguished depending on the initial film thickness. When the thickness is larger than a critical value, which in the case of Ni deposited on amorphous SiO_2 is 5 nm, the thermal annealing induces a grain size increase that causes the cluster agglomeration; for smaller thicknesses, the grain size increase is inhibited and the film is not able to break up into clusters. Of course, since our experiment is limited in temperature and time, we cannot exclude *a priori* that also films with a thickness less than 5 nm can agglomerate if annealed at higher temperature or for a longer time. The observed two-regime behavior should not be limited to our experimental case (Ni on SiO_2) but should have general validity, which invites future investigation of similar systems.

ACKNOWLEDGMENTS

We would like to thank all the staff of the 34–ID-C beamline at APS for their invaluable help during the measurements. The use of the APS was supported by the U.S. Department of Energy, Office of Science, Office of Basic Energy Sciences, under Contract No. DE-AC02-06CH11357.

[1] C. Favazza, R. Kalyanaraman, and R. Sureshkumar, Nanotechnology **17**, 4229 (2006).
[2] W. W. Mullins, Acta Metall. **6**, 414 (1958).
[3] R. Saxena, M. J. Frederick, G. Ramanath, W. N. Gill, and J. L. Plawsky, Phys. Rev. B **72**, 115425 (2005).
[4] H. C. Kim, N. D. Theodore, and T. L. Alford, J. Appl. Phys. **95**, 5180 (2004).
[5] A. L. Giermann and C. V. Thompson, Appl. Phys. Lett. **86**, 121903 (2005).
[6] B. Lamprecht, G. Schider, R. T. Lechner, H. Ditlbacher, J. R. Krenn, A. Leitner, and F. R. Aussenegg, Phys. Rev. Lett. **84**, 4721 (2000).
[7] S. A. Maier, P. G. Kik, H. A. Atwater, S. Meltzer, E. Harel, B. E. Koel, and A. A. G. Requicha, Nature Mater. **2**, 229 (2003).
[8] K. M. Ryu, M. Y. Kang, Y. D. Kim, and H. T. Jeon, Jpn. J. Appl. Phys. Part 1 **42**, 3578 (2003).
[9] W. D. Zhang, Y. Wen, S. M. Liu, W. C. Tjiu, G. Q. Xu, and L. M. Gan, Carbon **40**, 1981 (2002).
[10] C. Revenant, F. Leroy, R. Lazzari, G. Renaud, and C. R. Henry, Phys. Rev. B **69**, 035411 (2004); G. Renaud, R. Lazzari, C. Revenant, A. Barbier, M. Noblet, O. Ulrich, F. Leroy, J. Jupille, Y. Borensztein, C. R. Henry, J.-P. Deville, F. Scheurer, J. Mane-

Mane, and O. Fruchart, Science **300**, 1416 (2003).
[11] J.-Y. Kwon, T.-S. Yoon, Ki-B. Kim and S.-H. Min, J. Appl. Phys. **93**, 3270 (2003).
[12] L. Névot and P. Croce, Rev. Phys. Appl. **15**, 761 (1980).
[13] R. Lazzari, J. Appl. Crystallogr. **35**, 406 (2002).
[14] D. J. Srolovitz and S. A. Safran, J. Appl. Phys. **60**, 247 (1986); **60**, 255 (1986).
[15] T. P. Nolan, R. Sinclair, and R. Beyers, J. Appl. Phys. **71**, 720 (1992).
[16] E. Jiran and C. V. Thompson, Thin Solid Films **208**, 23 (1992).
[17] J. J. Rha and J. K. Park, J. Appl. Phys. **82**, 2933 (1997).
[18] J. J. Rha and J. K. Park, J. Appl. Phys. **82**, 1608 (1997).
[19] M. J. Rost, D. A. Quist, and J. W. M. Frenken, Phys. Rev. Lett. **91**, 026101 (2003).